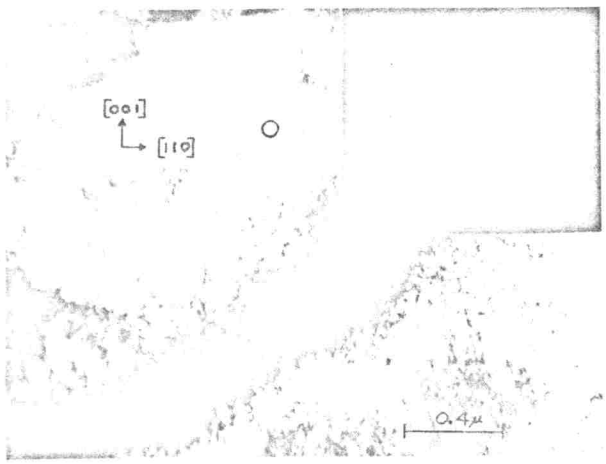

FIG. 8. Electron micrograph of shock-loaded Fe-7Mn at 300 kbar. Extensive transformation has occurred.

recognizable for the Fe-7Mn alloy [Figs. 4(b) and 4(c)]. This last observation is very important because it indicates that during shocking α' reverted to γ by the same mode of shear that occurred during quenching. In contrast to the case of Fe-7Mn, the austenitic grain boundaries in Fe-14Mn which existed prior to quenching are not visible after shocking because they are obscured by the α' to ϵ transformation. Consequently, the shocked Fe-14Mn is very nondescript. Figure 5(a) shows the structure of the slow-cooled Fe-7Mn alloy. This microstructure is typical for all slow-cooled alloys. The lightly outlined grains represent the hcp phase, while the matrix is the bcc phase. These phases have been identified by the electron probe and will be discussed in Sec. IV. Figure 5(b) shows the slow-cooled structure for Fe-7Mn after shock loading at 300 kbar. This microstructure is typical for all shocked furnace-cooled alloys. The prominent feature of the shocked furnace-cooled alloys is the presence of profuse twinning, and there is no retained high-pressure phase in the furnace-cooled specimens as supported by the density and x-ray observations.

The electron-probe microanalysis, while facilitating the interpretation of the optical micrographs, also indicated the distribution of manganese in the shocked and unshocked specimens. The manganese variation was measured in shocked specimens, and those which were only quenched or furnace cooled. Segregated regions were observed in both the 7 and 14 wt% Mn alloys furnace cooled from 900 °C. The type of segregation was the same in both the shocked and unshocked furnace-cooled specimens. The segregated regions in the furnace-cooled shock-loaded Fe-7Mn alloy were 5–15 μ long with manganese concentration changing discontinuously from 2.5 to 23.0 wt% [Fig. 6(a)]. Similarly segregated regions in the Fe-14Mn furnace-cooled shock-loaded specimens were also 5–15 μ long with a variation in manganese concentration from 3.5 to 40 wt% [Fig. 6(b)]. These variations are consistent with the manganese content in α and γ as predicted by the phase diagram. The manganese distribution in the quenched alloys was homogeneous and segregated regions were not detected. The quenched and then shocked alloys had the similar homogeneous distribution of manganese.

The microstructure of Fe-4Mn, Fe-7Mn, and Fe-14Mn was studied using the electron microscope. One alloy (Fe-7Mn) will be described in detail because its microstructure is representative of all alloys. The Fe-7Mn specimens which were shock loaded at 90 and 300 kbar showed fcc and bcc phases [Figs. 7(a) and 7(b)]. The fcc phase was identified by selected-area diffraction methods. The fcc phase was in the form of platelike islands of retained austenite within the martensite matrix. These plates of austenite were formed by shocking because no austenite existed in the as-quenched state. At 300 kbar, the amount of fcc was much greater as shown in Figure 7(b), as expected from the density measurements. On the other hand, the furnace-cooled Fe-7Mn specimens shocked to 90 kbar did not show retained fcc, as shown in Fig. 8, and were characterized primarily by a cellular dislocation structure. Shock loading the furnace-cooled specimens at 500 kbar resulted in the formation of subgrains indicating that some recovery had taken place during the shock loading.

The diffraction pattern of Fig. 7(a) (Fe-7Mn, 90 kbar) is primarily bcc resulting from the matrix. The fcc spots are marked on the pattern and indicate that the retained fcc cells are elongated in the same

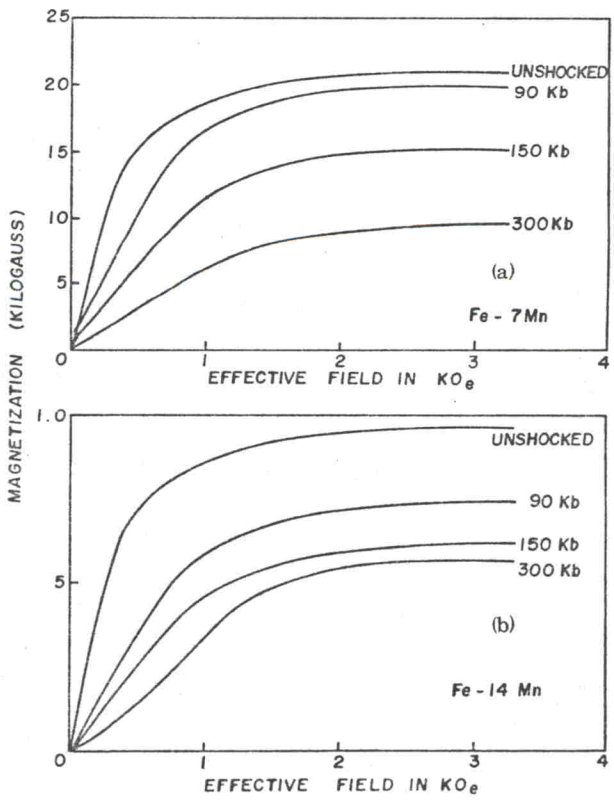

FIG. 9. Magnetization curves for shock-deformed Fe-Mn alloys: (a) Fe-7Mn and (b) Fe-14Mn.